The Matrix Protein of Human Parainfluenza Virus Type 3 Induces Mitophagy that Suppresses Interferon Responses

Binbin Ding,[1,2] Linliang Zhang,[1,2] Zhifei Li,[1] Yi Zhong,[1] Qiaopeng Tang,[1] Yali Qin,[1] and Mingzhou Chen[1,3,*]
[1]State Key Laboratory of Virology and Modern Virology Research Center, College of Life Sciences, Wuhan University, LuoJia Hill, Wuhan 430072, China
[2]Co-first author
[3]Lead Contact
*Correspondence: chenmz@whu.edu.cn
http://dx.doi.org/10.1016/j.chom.2017.03.004

SUMMARY

Mitophagy is a form of autophagy that selectively removes damaged mitochondria. Impaired mitochondria can be tagged by the kinase PINK1, which triggers recruitment of the E3-ubiquitin ligase Parkin and subsequent mitochondrial sequestration within autophagosomes. We previously found that human parainfluenza virus type 3 (HPIV3) infection induces autophagy, but the type and mechanisms of autophagy induction remain unknown. Here, we show that matrix protein (M) of HPIV3 translocates to mitochondria and interacts with Tu translation elongation factor mitochondrial (TUFM). M-mediated mitophagy does not require the Parkin-PINK1 pathway but rather an interaction between M and the LC3 protein that mediates autophagosome formation. These interactions with both TUFM and LC3 are required for the induction of mitophagy and lead to inhibition of the type I interferon response. These results reveal that a viral protein is sufficient to induce mitophagy by bridging autophagosomes and mitochondria.

INTRODUCTION

Mitophagy is a form of autophagy that selectively removes the mitochondria and is critical for controlling the number of functional mitochondria in the cell (Patergnani and Pinton, 2015). Mitochondrial sequestration by autophagosomes is a key step of mitophagy, which can be broadly classified into two distinct groups: Parkin dependent and Parkin independent. Parkin-dependent mitophagy involves selective tagging of damaged mitochondria by PTEN-induced putative kinase 1 (PINK1) followed by Parkin recruitment to the impaired mitochondria and subsequent mitophagy (Narendra et al., 2010), which generally is regulated by some mitophagy receptors, such as SQSTM1 (p62), NIX, NBR1, or TAX1BP1 (Aoki et al., 2011; Geisler et al., 2010; Zhang and Ney, 2009). These receptors are recruited to mitochondria via ubiquitin binding and mediate autophagic engulfment through their association with microtubule-associated protein light chain 3 (LC3). However, a recent study showed that OPTN and NDP52 are the only receptors required and sufficient to drive mitophagy, whereas other tested receptors appear to be dispensable for mitophagy (Lazarou et al., 2015).

The mitochondrial network is highly susceptible to viral infections and can be either directly targeted by viral proteins or influenced by the physiological alterations in the cellular environment during viral pathogenesis. For example, hepatitis B and hepatitis C viral infections can induce mitophagy for the maintenance of persistent infection (Kim et al., 2013a, 2013b, 2014). However, the mechanisms by which virus-induced mitophagy occurs and the molecular mechanisms responsible for the regulation of mitophagy during viral infection remain to be determined.

Human parainfluenza virus type 3 (HPIV3) is a member of the family Paramyxoviridae in the order Mononegavirales with a non-segmented negative-strand RNA genome, a genome that codes six structural proteins: nucleoprotein (N), phosphoprotein (P), polymerase (L), matrix protein (M), and two spike glycoproteins consisting of hemagglutinin-neuraminidase protein (H) and fusion protein (F). M plays a key role in directing viral assembly and budding by connecting the F and/or H and the RNPs (Zhang et al., 2014).

HPIV3 is one of the primary pathogens that causes severe respiratory tract diseases, including bronchiolitis, pneumonia, and croup, in infants and young children. However, no valid antiviral therapy or vaccine is currently available. Thus, further investigation of the effect of mitochondrial dynamics in HPIV3 infections will enhance our understanding of virus-host interactions and their role in pathogenesis, which will hold significant potential for developing effective antiviral therapy or vaccines in the near future.

In this study, we demonstrate that M of HPIV3 interacts with a mitochondrial Tu translation elongation factor (TUFM) to translocate to mitochondria and induce mitophagy, resulting in the inhibition of the type I interferon (IFN) response. Furthermore, we found that M associates with LC3 and functions as an autophagy receptor to mediate mitophagy.

RESULTS

HPIV3 Infection and M Expression Induce Mitophagy

Our previous study showed that HPIV3 infection induces incomplete autophagy by blocking autophagosome-lysosome fusion,
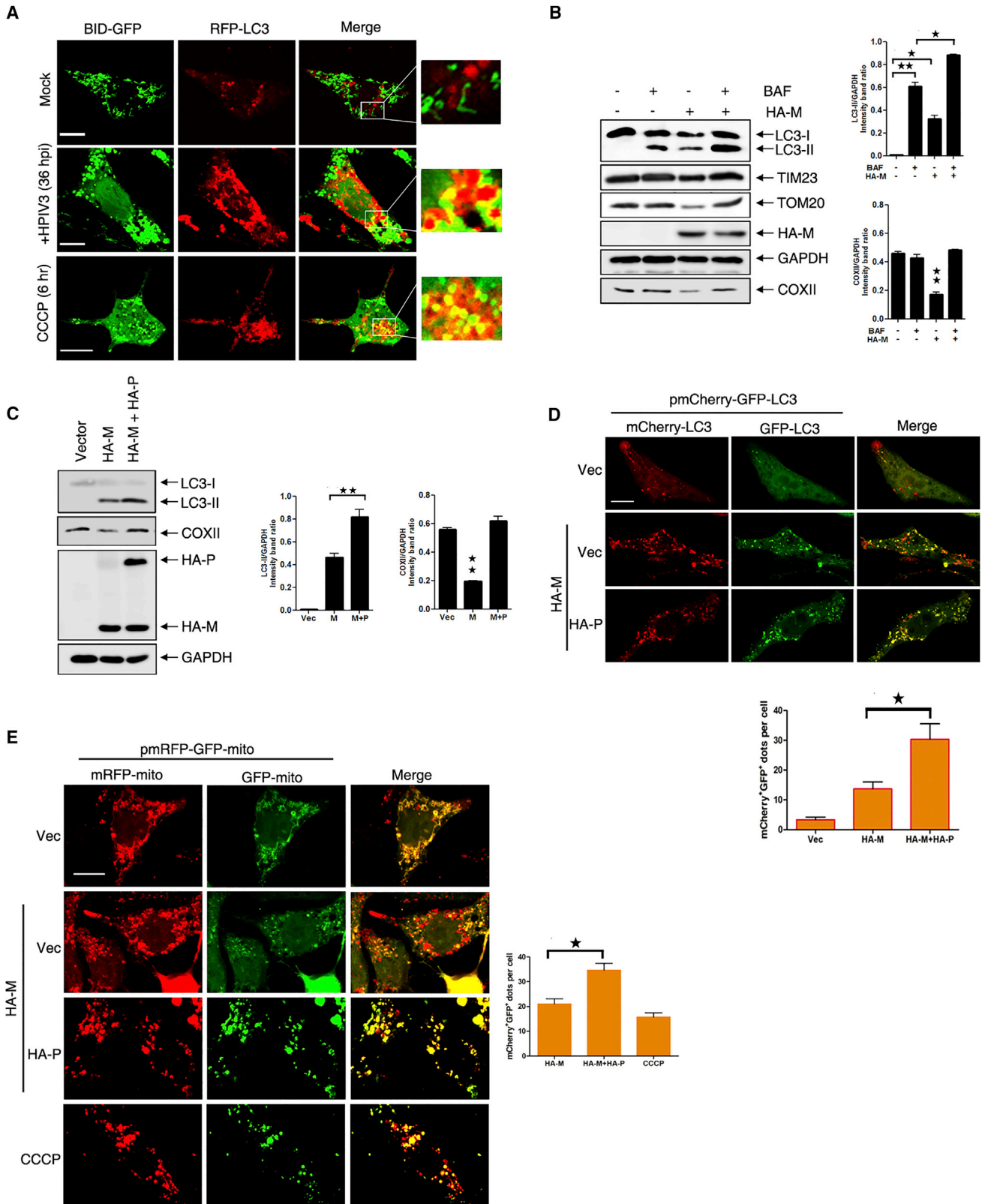
Figure 1. HPIV3 Infection and M Expression Induce Mitophagy

(A) HeLa cells were transfected with indicated plasmids and infected with HPIV3 for 36 hr or treated with CCCP for 6 hr and analyzed for the colocalization of RFP-LC3 and BID-GFP.

resulting in increased virus production, and the viral P is necessary and sufficient to inhibit autophagosome degradation. Next, we sought to determine which type of autophagy HPIV3 induces and the mechanism by which it induces autophagy. First, we found that red fluorescent protein (RFP)-tagged LC3 colocalized with green fluorescent protein (GFP)-tagged BH3 interacting domain death agonist (BID-GFP), a mitochondrial marker protein in HPIV3-infected cells, and we used carbonyl cyanide 3-chlorophenyl hydrazine (CCCP)-induced mitophagy as a positive control (Figure 1A), indicating that HPIV3 infection induced mitophagy. In addition, by using transmission electron microscopy, we were unable to clearly demonstrate a double membrane of autophagosomes, but representative electron micrographs suggested to us that this process was similar to conventional mitophagy (Figure S1A).

To determine whether HPIV3 infection induces incomplete mitophagy, we used a tandem reporter construct encoding a mitochondria-targeting signal sequence fused to RFP and EGFP gene, mRFP-EGFP-mito. The GFP signal is attenuated in an acidic pH environment, while RFP can be visualized in lower pH; therefore, the fusion of mitophagosomes with lysosomes results in the loss of yellow fluorescence and the appearance of only red fluorescence of RFP, indicating the completion of the mitophagic process (Kim et al., 2013a). In HPIV3-infected cells, yellow fluorescence derived from GFP and RFP that merged is observed in mitophagosomes, whereas in CCCP-treated cells, only red fluorescence remained (Figure S1B), indicating that mitophagosomes did not fuse with lysosomes in HPIV3-infected cells. Furthermore, HPIV3 infection also blocked CCCP-induced complete mitophagy and resulted in the enhancement of LC3-II via the accumulation of mitophagosomes (Figure S1C). Thus, HPIV3 infection induces incomplete mitophagy.

To clarify the mechanism(s) by which HPIV3 infection induces incomplete mitophagy, we transiently expressed N, P, M, F, and H of HPIV3, and M expression resulted in a significant decrease in the mitochondrial DNA-encoded inner membrane protein cytochrome C oxidase subunit II (COXII), which indicates complete mitophagy (Lazarou et al., 2015), suggesting that M induces complete mitophagy (Figure S1D). Furthermore, M expression resulted in RFP-LC3 colocalization with BID-GFP (Figure S1E), a decrease in outer membrane mitochondrial protein TOM20, inner membrane protein TIM23, p62 (an indicator of autophagic degradation), and COXII (Figure S1F). To further demonstrate specificity of M-induced mitophagy, we also examined the quantities of marker proteins of proteasome (PA28 and PSMA3) and ribosomes (L2a and RPL5) in the presence of M at different time points and found that M expression did not result in significant change of these protein levels, indicating that M-induced autophagosomes are devoid of proteasomes and ribosomes (Figure S1G).

Most importantly, the decrease in p62, COXII, and mitochondrial proteins induced by M was prevented by bafilomycin A1 (BAF, a pharmacologic inhibitor of the activity of lysosomes) (Figure 1B). We also found that higher levels of LC3-II were accumulated in the presence of M than in the absence of M upon BAF treatment (Figure 1B); similarly, the degradation of COXII caused by M was prevented in the presence of P (Figure 1C). Furthermore, we also used the plasmid mCherry-GFP-LC3 and found that a high number of mCherry-positive autolysosomes remained detectable, and only small proportion of the LC3-positive autophagic vacuoles was yellow in M-expressing cells. While in cells co-expressing M and P cells, many LC3-positive autophagic vacuoles were yellow (Figure 1D). Similarly, in mRFP-EGFP-mito transfected cells, yellow fluorescence disappeared, and only the red fluorescence of RFP appeared in M-expressing cells, as in CCCP-treated cells, suggesting that M expression induces complete mitophagy (Kim et al., 2013a). Substantial yellow fluorescence, indicating the presence of GFP- and RFP-positive mitophagosomes, was observed in cells expressing mRFP-EGFP-mito, M, and P (Figure 1E), suggesting that M expression induces complete mitophagy, and P blocks the fusion of mitophagosomes with lysosomes and subsequent degradation, resulting in the accumulation of mitophagosomes.

M Interacts with TUFM

Next, we sought to determine the mechanism(s) by which M induces complete mitophagy. We expressed M as a bait and then performed in vivo immunoprecipitation (IP), followed by mass spectrometry (MS) analysis. TUFM was shown to interact with M by reciprocal coIP experiments (Figures 2A–2C). Furthermore, we performed an in vitro glutathione S-transferase (GST) pulldown assay with GST-fused M expressed in HEK293T cells. GST-M, but not GST alone, was able to pull down TUFM (Figure S2A). Furthermore, endogenous TUFM coimmunoprecipitated with Myc-M in HEK293T cells (Figure 2D) and colocalized with M-GFP in HeLa cells via immunofluorescence assay (Figure S2B). Taken together, these results confirm that M and TUFM physically interact in vivo and in vitro.

Next, to map the critical region in TUFM necessary for its interaction with M, we constructed a series of TUFM-deleted mutants (Lei et al., 2012) and used them for a coIP assay. We found that mutant with domain II deleted barely coimmunoprecipitated with Myc-M, whereas mutant with domain I and III deleted still interacted with Myc-M as efficiently as TUFM (Figure S2C), suggesting domain II is indeed required for regulating the interaction of TUFM with M. To map the domains in M that are essential for its interaction with TUFM, we constructed a series of truncated mutants of M. The deletion of the C terminus of 40 residues (M△C40) definitely abolished the interaction of M with Flag-TUFM, suggesting that the C-terminal 40 residues are

---

(B) HeLa cells were transfected with HA-M for 30 hr and treated with BAF and analyzed via WB.

(C) HeLa cells were transfected with HA-P and HA-M. Lysates were evaluated via WB.

(D) HeLa cells were transfected with pmCherry-GFP-LC3, HA-M, and HA-P for 30 hr and then analyzed to detect autophagosomes. Scale bar, 10 μm. The graph shows the quantification of autophagosomes by taking the average number of dots in 50 cells.

(E) HeLa cells were transfected with pmRFP-GFP-mito, HA-M, and HA-P for 30 hr, then treated with CCCP, and then analyzed to detect mitophagosomes. Scale bar, 10 μm. The graph shows the quantification of mRFP$^+$GFP$^+$ mitophagosomes by taking the average number of dots in 50 cells (n = average number of dots in 50 cells).

Error bars, mean ± SD of three experiments (n = 3). Student's t test; *p < 0.05; **p < 0.01; ***p < 0.001. See also Figure S1.
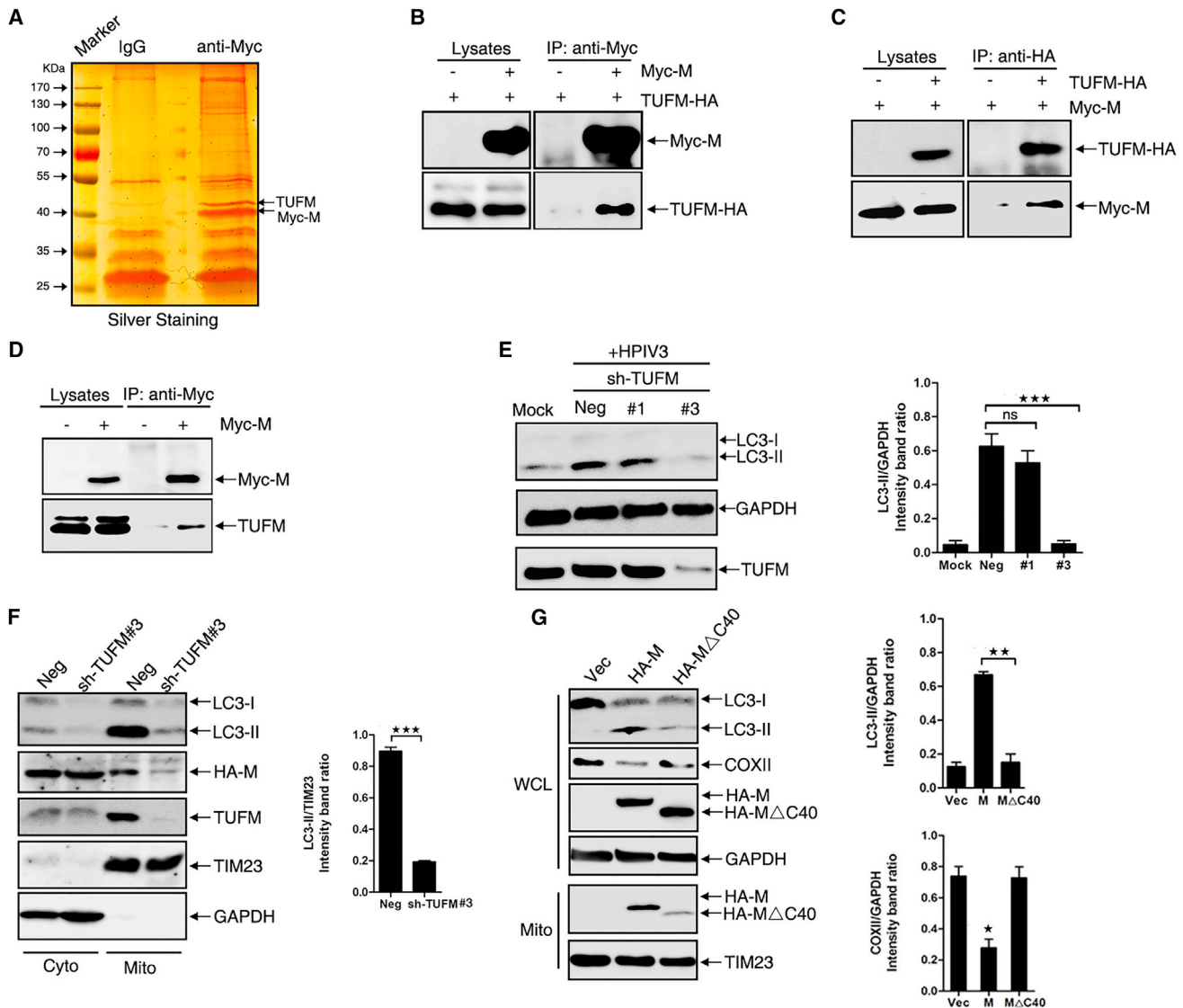
Figure 2. M Interacts with TUFM and Induces TUFM-Dependent Mitophagy

(A) HEK293T cells were transfected with Myc-M for 48 hr. Lysates were subjected to IP/MS and eluted proteins were separated via SDS-PAGE and analyzed via silver staining.

(B) HEK293T cells were transfected with plasmids encoding Myc-M and TUFM-HA. Lysates were subjected to IP and analyzed via WB.

(C) HEK293T cells were transfected with plasmids encoding Myc-M and TUFM-HA. Lysates were subjected to IP and analyzed via WB.

(D) HEK293T cells were transfected with a plasmid encoding Myc-M, and lysates were subjected to IP and analyzed to detect endogenous TUFM via WB.

(E) A549 cells were transfected with sh-TUFM or sh-negative (Neg), and 24 hr later, cells were mock-infected or infected with HPIV3 (MOI = 0.01). Cells were harvested and analyzed via WB.

(F) HeLa cells were transfected with HA-M. Cytoplasm and mitochondrial fractions were isolated via ultracentrifugation. Cytoplasm (Cyto) and mitochondrial fractions (Mito) of sh-Neg or sh-TUFM transfected cells were analyzed via WB.

(G) HeLa cells were transfected with HA-M or HA-M △C40 for 30 hr, and mitochondrial fractions were isolated via ultracentrifugation. Whole-cell lysates (WCL) and mitochondrial fractions were analyzed via WB.

Error bars, mean ± SD of three experiments (n = 3). Student's t test; *p < 0.05; **p < 0.01; ***p < 0.001; ns, non-significant. See also Figure S2.

indeed required for regulating the interaction of M with TUFM (Figure S2D).

M Mediates TUFM-Dependent Mitophagy

A previous study showed that TUFM regulates vesicular stomatitis virus-induced autophagy (Lei et al., 2012). To determine whether TUFM also regulates HPIV3-induced autophagy, we

knocked down TUFM and found that LC3-II was significantly decreased compared with negative short hairpin RNA (shRNA) in HPIV3-infected cells (Figure 2E), indicating that TUFM regulates HPIV3-induced autophagy. Next, to determine whether TUFM also regulates HPIV3- and M-induced mitophagy, we transfected cells with GFP-LC3 and short hairpin (sh)-TUFM and then infected with HPIV3. GFP-LC3 signals of vacuole-like

structures were prominent and colocalized with TUFM (which is a mitochondrial protein) in negative shRNA-treated cells but was less prominent in TUFM-knockdown cells (Figure S2E). Similar results were observed when M was expressed with negative shRNA-treated or TUFM knockdown cells, indicating that TUFM is also required for M-induced mitophagy (Figure S2F).

To confirm that M mediates TUFM-dependent mitophagy, we analyzed autophagy in cytosolic fractions and mitochondria-enriched fractions. For this purpose, we first ensured that separating mitochondrial fractions from cytosolic fractions was feasible via analysis of GFP (which exists in cytosolic fractions) and TIM23 (which exists in mitochondrial fractions) (Figure S2G). Cell lysates expressing M with sh-TUFM displayed significantly reduced LC3-II and M in mitochondria-enriched fractions compared to negative shRNA (Figure 2F), suggesting that TUFM is necessary to recruit M to the mitochondria and is critical for M-induced mitophagy. Furthermore, the M mutant M △ C40 lacking the TUFM-interaction domain did not degrade COXII either (Figure 2G), suggesting that the interaction of TUFM and M is critical for M-induced mitophagy. To further demonstrate that TUFM is a specific regulator of M-induced mitophagy, we also performed rescue experiments in the TUFM knockdown cells and found that wild-type TUFM, but not TUFM △ II, rescued the conversion of LC3-I into LC3-II and reduced the expression of TIM23, TOM20, and COXII (Figure S2H). Taken together, these results show that TUFM interaction with M is required for recruiting M to mitochondria and for M-induced mitophagy.

M Inhibits Mitophagy-Dependent Type I IFN Response

It has been known that RNA viruses are recognized by RIG-I-like receptors (RLRs) upon infecting cells and then RLRs interact with mitochondrial antiviral signaling protein (MAVS/IPS-1/VISA) to activate the type I IFN response. Having established that M can induce mitophagy, resulting in mitochondrial sequestration by autophagosomes, we thought to determine whether M expression will block type I IFN response; thus, we assessed the ability of M to inhibit IFN production using a plasmid containing a reporter gene (luciferase) under the control of an IFN-β promoter. We found that the N terminus of RIG-I (RIG-I-N)- or Sendai virus-activated IFN-β promoter-driven luciferase activity was dramatically inhibited by M in a dose-dependent manner (Figures 3A and 3B). Quantitative reverse transcriptase polymerase chain reaction (qRT-PCR) analysis of cellular mRNAs in response to RIG-I-N activation also demonstrated that M potently inhibited the production of IFN-β (Figure 3C), suggesting that M has the unique ability to downregulate IFN response. Furthermore, M could also inhibit type I IFN response upon RIG-I stimulation in the presence of P in similar level with M expression alone, which suggested incomplete mitophagy was also able to suppress type I IFN responses (Figure 3D). However, knockdown TUFM by sh-TUFM#3 abolished the inhibitory effect of M on IFN-β mRNA production triggered by RIG-I-N (Figure 3E), and M △ C40 also failed to inhibit IFN-β mRNA production triggered by RIG-I-N (Figure 3F), suggesting that the inhibition of type I IFN response by M depends on the interaction of M with TUFM. Furthermore, knockdown of autophagy-related genes Atg5 and Atg7 completely eliminated the effect of M on the type I IFN response (Figures 3G and 3H). Taken together,

our data show that M inhibits mitophagy-dependent type I IFN response.

M Interacts with LC3 and Acts as a Receptor of Mitophagy

Having established that M-induced mitophagy inhibits type I IFN response via mitochondrial sequestration by autophagosomes, we sought to determine how M regulates mitochondrial sequestration by autophagosomes, resulting in mitophagy. Our previous study showed that M colocalizes with GFP-LC3 (Ding et al., 2014), indicating that M may interact with LC3. Therefore, we carried out coIP assays to determine whether M interacts with LC3. As expected, M did physically interact with HA-LC3 (Figure 4A) and GFP-LC3 (Figure 4B), and endogenous LC3 also coimmunoprecipitated with Myc-M in HEK293T cells (Figure 4C). Furthermore, we performed an in vitro GST pull-down assay with GST-fused M expressed in HEK293T cells. GST-M, but not GST alone, was able to pull down GFP-LC3 (Figure S3A).

Some proteins that interact with LC3 can function as mitophagy receptors and contain a typical linear motif with the conserved sequence of W/YxxL/I (Noda et al., 2010; Pankiv et al., 2007), but there is no classical W/YxxL/I motif in M. Thus, we sought to map the critical region in M necessary for its interaction with LC3 using a series of M-deleted mutants for coIP assays. Deletion of C terminus of 41–80 residues of M (M △ C41–80) remarkably impaired M association with LC3 (Figure 4D; Figure S3B). Furthermore, M △ C41–80 also failed to induce mitophagy (Figure 4E), which is similar to the results with M △ C40, suggesting that the association of M with LC3 is also critical for M-induced mitophagy.

Next, we further identified a critical amino acid within M C terminus of 41–80 residues—K295—and found that M_{K295A} neither interacted with GFP-LC3 (Figure 4F) nor induced mitophagy (Figure 4G), but interacted with TUFM (Figure S3D), suggesting that K295 is critical for the interaction of M with LC3 and for M-induced mitophagy. To exclude the possibility that other autophagy-related proteins mediate M-LC3 interaction, we performed a coIP assay and found that only endogenous LC3, but not other autophagic proteins (p62, Atg5, Atg7, and Beclin1), interacted with M (Figure S3E). In addition, M still induced mitophagy when mitophagy receptor NDP52 was knocked down (Figure S3F), and NDP52 also did not interact with M (Figure S3G).

Furthermore, only M, not M_{K295A}, interacted with endogenous LC3 (Figure S3E). We also expressed BID-GFP and RFP-LC3 with M or its mutants and found that M induced prominent LC3-RFP-positive vacuole-like signals that colocalized with BID-GFP and M, but neither M △ C40, M △ C41-80, nor M_{K295A} induced colocalization of LC3-RFP-positive vacuole-like signals with BID-GFP (Figure S3H), suggesting that M-induced mitophagy requires its interaction with TUFM and interaction with LC3. Furthermore, M △ C40, M △ C41-80, and M_{K295A} failed to inhibit *ifnb1* mRNA production triggered by RIG-I-N (Figure S3I).

Our previous study showed that M is ubiquitinated (Zhang et al., 2014). Thus, we sought to know whether ubiquitination influences M interaction with LC3 and found that ubiquitination of M_{K295A} was decreased (Figure 4H). Furthermore, treatment of cells with MG132, which decreases free ubiquitin, decreased the interaction of M with LC3 (Figure 4I) but did not influence
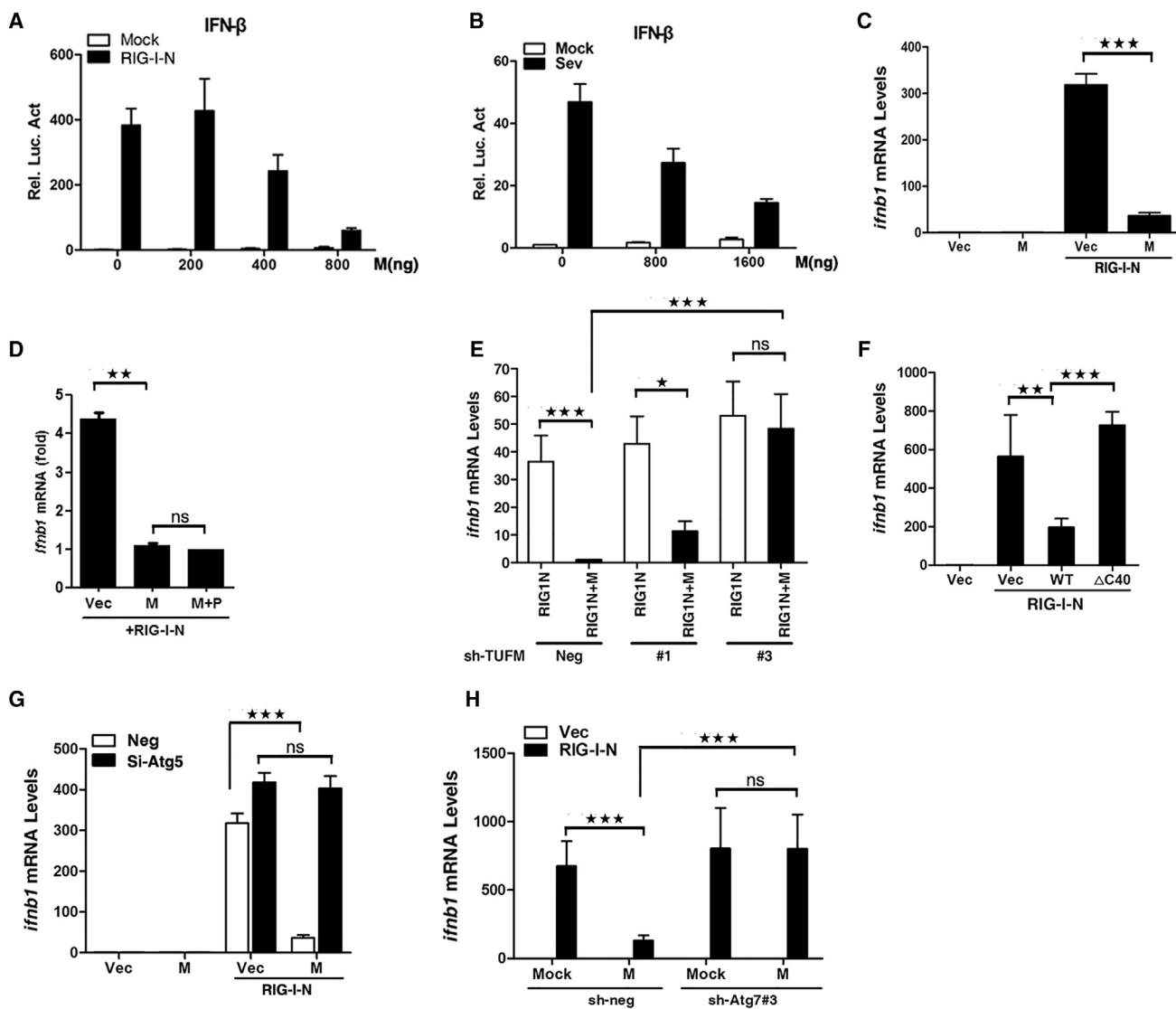
Figure 3. M Inhibits the Type I IFN Response Dependent on TUFM and Mitophagy

(A) HEK293T cells were transfected with indicated plasmids. Reporter assays were performed 24 hr after transfection.

(B) HEK293T cells were transfected with indicated plasmids, and 24 hr later, cells were further mock-infected or infected with Sendai virus for another 8 hr before reporter assays were performed.

(C) HEK293T cells were transfected with indicated plasmids. RNAs were isolated from cells and reverse transcribed. The levels of *ifnb1* mRNA were measured via real-time PCR.

(D) HEK293T cells were transfected with indicated plasmids. The levels of *ifnb1* mRNA were measured via real-time PCR.

(E) HEK293T cells were transfected with sh-TUFM, and 24 hr later, cells were further transfected with indicated plasmids. The levels of *ifnb1* mRNA were measured via real-time PCR.

(F) HEK293T cells were transfected with indicated plasmids. RNAs were isolated from cells and reverse transcribed. The levels of *ifnb1* mRNA were measured via real-time PCR.

(G and H) HEK293T cells were transfected with sh-Atg5 (G) or sh-Atg7 (H), and 24 hr later, cells were further transfected with indicated plasmids. The levels of *ifnb1* mRNA were measured as (E).

Error bars, mean ± SD of three experiments (n = 3). Student's t test; *p < 0.05; **p < 0.01; ***p < 0.001; ns, non-significant.

the interaction of M with TUFM (Figure S3C), suggesting that ubiquitinated M might bind preferentially to LC3.

Because mitophagy is generally PINK1 dependent, and Parkin can ubiquitinate mitochondrial substrates to amplify the mitophagy signal (Lazarou et al., 2015), we sought to determine whether PINK1 or Parkin are also required for M-induced mitophagy.

Because HeLa cells do not express endogenous Parkin (Lazarou et al., 2015), M-induced mitophagy in HeLa cells suggests that M can induce mitophagy in the absence of Parkin. Furthermore, overexpression of Parkin in HeLa cells had no effect on the ubiquitination of M (Figure S3J), suggesting that Parkin does not function in M-induced mitophagy. In addition, we found that
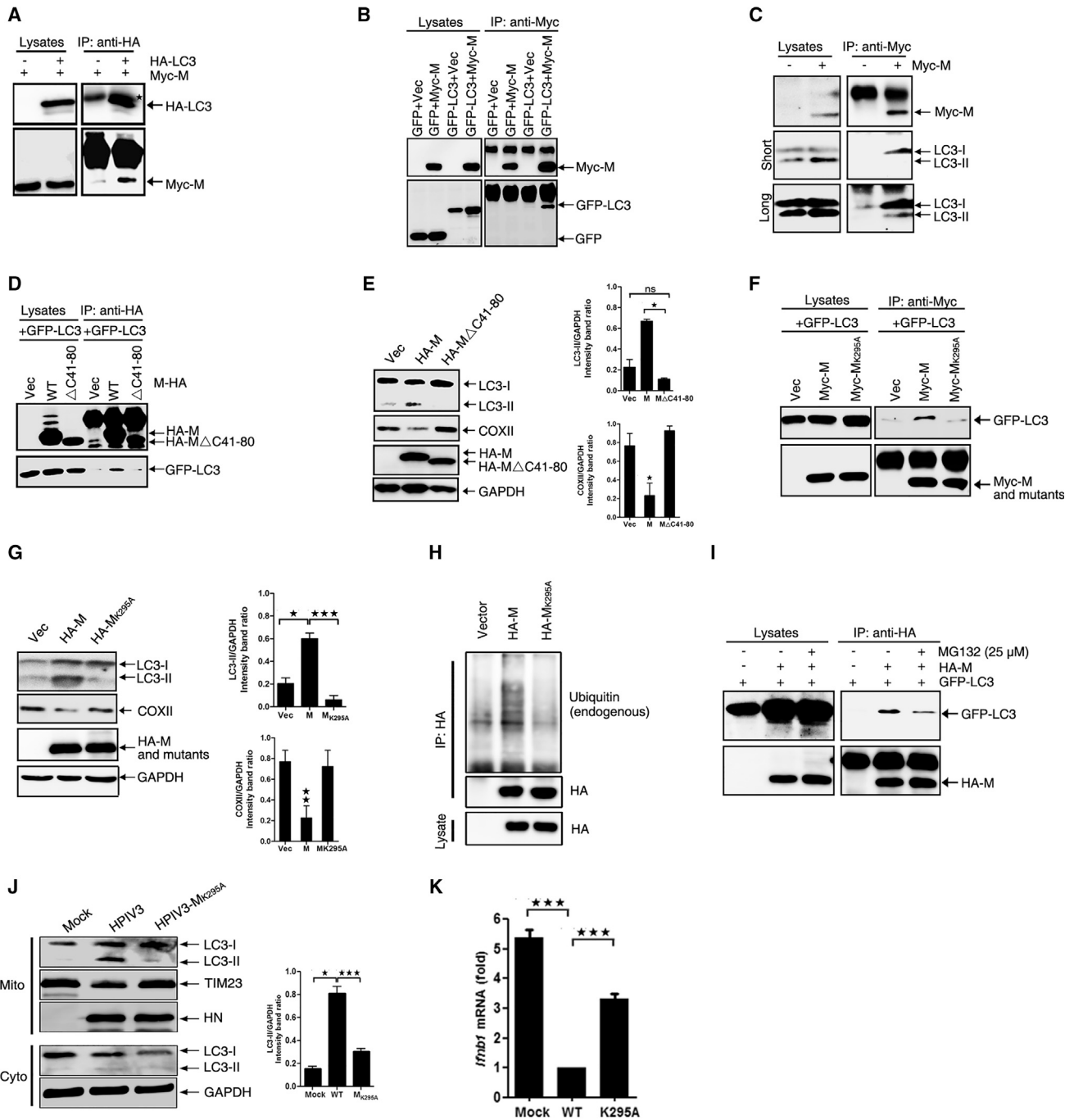
Figure 4. M Acts as a Receptor to Interact with LC3

(A) HEK293T cells were transfected with Myc-M alone or with both Myc-M and HA-LC3. Cell lysates were subjected to IP and analyzed via WB.

(B) HEK293T cells were transfected with GFP-LC3 or GFP alone or co-expressed with Myc-M. Cell lysates were subjected to IP and analyzed via WB.

(C) HEK293T cells were transfected with plasmid encoding Myc-M, and lysates were subjected to IP using anti-Myc Ab to detect endogenous LC3.

(D) HA-M and HA-M △ C41-80 were co-expressed with GFP-LC3. Cell lysates were subjected to IP and analyzed via WB.

(E) HeLa cells were transfected with HA-M and HA-M △ C41-80. Cell lysates were analyzed via WB.

(F) HEK293T cells were transfected with GFP-LC3 alone or co-expressed with Myc-M or Myc-M$_{K295A}$. Lysates were subjected to IP and analyzed via WB.

(G) HeLa cells were transfected with HA-M and HA-M$_{K295A}$. Cell lysates were analyzed via WB.

(H) HEK293T cells were transfected with plasmids encoding HA-M and HA-M$_{K295A}$ and lysates were subjected to IP and analyzed to detect endogenous ubiquitin via WB.

(I) HEK293T cells were transfected with GFP-LC3 alone or with both GFP-LC3 and HA-M. Cells were treated with MG132 for another 6 hr. Lysates were subjected to IP and analyzed via WB.

(legend continued on next page)

CCCP treatment, but not M expression, significantly increased PINK1 expression in HeLa cells. (Figure S3K). Also, M could induce mitophagy even when PINK1 was knocked down (Figure S3L). Taken together, these results suggest that M acts as a receptor to mediate mitophagy independent of the Parkin-PINK1 pathway.

Recombinant HPIV3-M$_{K295A}$ Fails to Induce Mitophagy

Since M$_{K295A}$ neither interacted with LC3 nor induced mitophagy when expressed alone. In order to assure that K295 is responsible for M-induced mitophagy in infection, we successfully rescued the recombinant HPIV3 containing M$_{K295A}$ mutation and confirmed that the full length of the genome sequence of the mutant virus and its titer was at least 10-fold lower than that of wild-type HPIV3 (Figure S4A) and that HN expression of HPIV3-M$_{K295A}$ was lower than that of wild-type HPIV3 only at the early infection phase but was comparable at the later infection phase (Figure S4B).

Then, we performed functional assays and found that LC3-RFP barely colocalized with BID-GFP in HPIV3-M$_{K295A}$-infected cells either (Figure S4C), suggesting that HPIV3-M$_{K295A}$ failed to induce mitophagy. To further confirm this, we also examined autophagy in cytosolic and mitochondria-enriched fractions after 48 hr infection. In mitochondria-enriched fractions, we found that LC3-II was dramatically reduced in HPIV3-M$_{K295A}$-infected cells compared to that in wild-type HPIV3-infected cells, but there was no difference of LC3-II in cytosolic fractions between wild-type and HPIV3-M$_{K295A}$ (Figure 4J).

Next, we sought to verify whether HPIV3-M$_{K295A}$ reduced the ability to inhibit the type I IFN response. As expected, HPIV3-M$_{K295A}$ greatly lost the ability to inhibit the type I IFN response triggered by RIG-I-N compared to wild-type HPIV3 at a low MOI (Figure 4K). Taken together, our results show that K295 within M indeed was critical to HPIV3-induced mitophagy.

DISCUSSION

In this study, through IP/MS, we identified TUFM as a partner of M and clarified that M-induced mitophagy and the translocation of M into mitochondria rely on its interaction with TUFM. Furthermore, we also demonstrated that M-induced mitophagy inhibits mitochondrial-mediated innate immune responses (Figure 3). A similar study also showed that influenza A virus protein PB1-F2 translocates into mitochondria, accelerates mitochondrial fragmentation, and suppresses the RIG-I signaling pathway (Yoshizumi et al., 2014). Subsequently, we found that the interaction of M with LC3 is required for M-induced mitophagy, and M$_{K295A}$ neither interacts with LC3 nor induces mitophagy (Figure 4). Furthermore, recombinant HPIV3-M$_{K295A}$ fails to induce mitophagy (Figure 4; Figure S4).

Given the findings of our previous study and the present study, we propose the following model (Figure S4H): in HPIV3-infected cells, M translocates into mitochondria via its interaction with TUFM, and M mediates mitochondrial sequestration by auto-

phagosomes via its interaction with LC3, resulting in mitophagy; the subsequent fusion of mitophagosomes with lysosomes is blocked by P, which, on one hand, interferes with the RIG-I signaling pathway and, on the other hand, could be directly profitable for the viral infection by providing membranous assembly or transportation platforms (Ding et al., 2014).

Generally, PINK1 can phosphorylate ubiquitin chains on mitochondria and recruit autophagy receptors, such as NDP52 and OPTN, to induce mitophagy, which require PINK1 kinase activity and ubiquitin-binding domains of the receptors (Lazarou et al., 2015; Richter et al., 2016). Here, we found that M-induced mitophagy is independent of both Parkin and PINK1 since the absence of Parkin and PINK1 had no effect on M-induced mitophagy (Figure S3). Recent studies have shown that other ubiquitin ligases, such as FBXO7 and MUL1, act in parallel to Parkin in mitophagy (Burchell et al., 2013; Yun et al., 2014), and ULK1 translocates to the mitochondria and phosphorylates FUNDC1 to regulate mitophagy by direct binding to LC3 (Wu et al., 2014). Other studies have suggested the existence of PINK1-Parkin-independent pathways of mitophagy. For example, iron chelation was shown to induce mitophagy independent of PINK1 stabilization and Parkin activation in primary human fibroblasts as well as those isolated from Parkinson's disease patients with Parkin mutations (Allen et al., 2013); moreover, AMBRA1 is present at the mitochondria and able to induce mitophagy via LC3 binding, independent of Parkin (Strappazzon et al., 2015). Of note, we cannot exclude the possibilities that other proteins in mitochondria may also facilitate the recruitment of M to mitochondria, and unknown cellular proteins may act as adaptor proteins that bind to M ubiquitin chains to bridge the interaction of M with LC3, thereby recruiting mitochondria to autophagosomes.

A previous study showed that Edmonston vaccine strain measles virus infection can induce different types of autophagy that play multiple roles. Common autophagy may directly enhance Edmonston vaccine strain measles virus replication (Grégoire et al., 2011; Richetta et al., 2013), while mitophagy promotes viral replication by the attenuation of the innate immune response (Xia et al., 2014). In this study, we found that in the VISA knockout (Visa$^{-/-}$) mouse embryonic fibroblast cells (MEFs) (Li et al., 2012; Xu et al., 2012) (Figure S4D), in which type I IFN response was abrogated, HPIV3-M$_{K295A}$ virus replication was significantly increased compared to that in Visa$^{+/+}$ MEFs (Figure S4E), suggesting that compromised type I IFN production by mitochondrial sequestration is important for the replication of HPIV3. However, in Visa$^{-/-}$ MEFs, replication levels of HPIV3-M$_{K295A}$ was still lower than that of wild-type HPIV3 (Figure S4F). Furthermore, we also found that replication of HPIV3-M$_{K295A}$ could be significantly increased by CCCP treatment (Figure S4G). Therefore, we thought virus-induced incomplete mitophagy contributed to viral replication by providing autophagic membranes and inhibiting the type I response.

In summary, our study demonstrates a previously unappreciated role for a viral protein that acts as a receptor to mediate

---

(J) HeLa cells were mock infected or infected with wild-type HPIV3 and HPIV3-M$_{K295A}$. At 48 hr postinfection, cell lysates of cytoplasm and mitochondrial fractions were isolated by ultracentrifugation and analyzed via WB.

(K) HEK293T cells were transfected with indicated plasmids. At 12 hr posttransfection, cells were further mock infected or infected with wild-type HPIV3 and HPIV3-M$_{K295A}$ (MOI = 0.1) for 30 hr. The *ifnb1* mRNA was measured via qPCR.

Error bars, mean ± SD of three experiments (n = 3). Student's t test; *p < 0.05; **p < 0.01; ***p < 0.001; ns, non-significant.

mitophagy independent of the Parkin-PINK1 pathway and reveals the functional importance of M in autophagy during HPIV3 infection.

STAR★METHODS

Detailed methods are provided in the online version of this paper and include the following:

- KEY RESOURCES TABLE
- CONTACT FOR REAGENT AND RESOURCE SHARING
- METHOD DETAILS
  - Antibodies and Reagents
  - Cell Cultures
  - SDS-PAGE and Western Blot
  - Plasmids and siRNA Oligonucleotides
  - IP/MS
  - Subcellular Fractionation
  - Immunofluorescence Analysis
  - In Vivo CoIP
  - GST Pull-Down Assays
  - Transmission Electron Microscopy
  - Rescue and Characterization of Recombinant HPIV3-M_{K295A}
- QUANTIFICATION AND STATISTICAL ANALYSIS
- DATA AND SOFTWARE AVAILABILITY

AUTHOR CONTRIBUTIONS

B.D., L.Z., Y.Q., and M.C. designed the experiments, analyzed and organized data, and wrote the paper; B.D., L.Z., and Z.L. performed the experiments; Y.Z. helped construct mutants and shRNAs; and Q.T. found that M could inhibit type I response triggered by RIG-I-N. All authors discussed the results and commented on the manuscript.

REFERENCES

Allen, G.F., Toth, R., James, J., and Ganley, I.G. (2013). Loss of iron triggers PINK1/Parkin-independent mitophagy. EMBO Rep. *14*, 1127–1135.

Aoki, Y., Kanki, T., Hirota, Y., Kurihara, Y., Saigusa, T., Uchiumi, T., and Kang, D. (2011). Phosphorylation of Serine 114 on Atg32 mediates mitophagy. Mol. Biol. Cell *22*, 3206–3217.

Burchell, V.S., Nelson, D.E., Sanchez-Martinez, A., Delgado-Camprubi, M., Ivatt, R.M., Pogson, J.H., Randle, S.J., Wray, S., Lewis, P.A., Houlden, H., et al. (2013). The Parkinson's disease-linked proteins Fbxo7 and Parkin interact to mediate mitophagy. Nat. Neurosci. *16*, 1257–1265.

Ding, B., Zhang, G., Yang, X., Zhang, S., Chen, L., Yan, Q., Xu, M., Banerjee, A.K., and Chen, M. (2014). Phosphoprotein of human parainfluenza virus type 3 blocks autophagosome-lysosome fusion to increase virus production. Cell Host Microbe *15*, 564–577.

Geisler, S., Holmström, K.M., Skujat, D., Fiesel, F.C., Rothfuss, O.C., Kahle, P.J., and Springer, W. (2010). PINK1/Parkin-mediated mitophagy is dependent on VDAC1 and p62/SQSTM1. Nat. Cell Biol. *12*, 119–131.

Grégoire, I.P., Richetta, C., Meyniel-Schicklin, L., Borel, S., Pradezynski, F., Diaz, O., Deloire, A., Azocar, O., Baguet, J., Le Breton, M., et al. (2011). IRGM is a common target of RNA viruses that subvert the autophagy network. PLoS Pathog. *7*, e1002422.

Kim, S.J., Khan, M., Quan, J., Till, A., Subramani, S., and Siddiqui, A. (2013a). Hepatitis B virus disrupts mitochondrial dynamics: induces fission and mitophagy to attenuate apoptosis. PLoS Pathog. *9*, e1003722.

Kim, S.J., Syed, G.H., and Siddiqui, A. (2013b). Hepatitis C virus induces the mitochondrial translocation of Parkin and subsequent mitophagy. PLoS Pathog. *9*, e1003285.

Kim, S.J., Syed, G.H., Khan, M., Chiu, W.W., Sohail, M.A., Gish, R.G., and Siddiqui, A. (2014). Hepatitis C virus triggers mitochondrial fission and attenuates apoptosis to promote viral persistence. Proc. Natl. Acad. Sci. USA *111*, 6413–6418.

Lazarou, M., Sliter, D.A., Kane, L.A., Sarraf, S.A., Wang, C., Burman, J.L., Sideris, D.P., Fogel, A.I., and Youle, R.J. (2015). The ubiquitin kinase PINK1 recruits autophagy receptors to induce mitophagy. Nature *524*, 309–314.

Lei, Y., Wen, H., Yu, Y., Taxman, D.J., Zhang, L., Widman, D.G., Swanson, K.V., Wen, K.W., Damania, B., Moore, C.B., et al. (2012). The mitochondrial proteins NLRX1 and TUFM form a complex that regulates type I interferon and autophagy. Immunity *36*, 933–946.

Li, Y., Chen, R., Zhou, Q., Xu, Z., Li, C., Wang, S., Mao, A., Zhang, X., He, W., and Shu, H.B. (2012). LSm14A is a processing body-associated sensor of viral nucleic acids that initiates cellular antiviral response in the early phase of viral infection. Proc. Natl. Acad. Sci. USA *109*, 11770–11775.

Malovannaya, A., Li, Y., Bulynko, Y., Jung, S.Y., Wang, Y., Lanz, R.B., O'Malley, B.W., and Qin, J. (2010). Streamlined analysis schema for high-throughput identification of endogenous protein complexes. Proc. Natl. Acad. Sci. USA *107*, 2431–2436.

Narendra, D.P., Jin, S.M., Tanaka, A., Suen, D.F., Gautier, C.A., Shen, J., Cookson, M.R., and Youle, R.J. (2010). PINK1 is selectively stabilized on impaired mitochondria to activate Parkin. PLoS Biol. *8*, e1000298.

Noda, N.N., Ohsumi, Y., and Inagaki, F. (2010). Atg8-family interacting motif crucial for selective autophagy. FEBS Lett. *584*, 1379–1385.

Pankiv, S., Clausen, T.H., Lamark, T., Brech, A., Bruun, J.A., Outzen, H., Øvervatn, A., Bjørkøy, G., and Johansen, T. (2007). p62/SQSTM1 binds directly to Atg8/LC3 to facilitate degradation of ubiquitinated protein aggregates by autophagy. J. Biol. Chem. *282*, 24131–24145.

Patergnani, S., and Pinton, P. (2015). Mitophagy and mitochondrial balance. Methods Mol. Biol. *1241*, 181–194.

Richetta, C., Grégoire, I.P., Verlhac, P., Azocar, O., Baguet, J., Flacher, M., Tangy, F., Rabourdin-Combe, C., and Faure, M. (2013). Sustained autophagy contributes to measles virus infectivity. PLoS Pathog. *9*, e1003599.

Richter, B., Sliter, D.A., Herhaus, L., Stolz, A., Wang, C., Beli, P., Zaffagnini, G., Wild, P., Martens, S., Wagner, S.A., et al. (2016). Phosphorylation of OPTN by TBK1 enhances its binding to Ub chains and promotes selective autophagy of damaged mitochondria. Proc. Natl. Acad. Sci. USA *113*, 4039–4044.

Strappazzon, F., Nazio, F., Corrado, M., Cianfanelli, V., Romagnoli, A., Fimia, G.M., Campello, S., Nardacci, R., Piacentini, M., Campanella, M., and Cecconi, F. (2015). AMBRA1 is able to induce mitophagy via LC3 binding, regardless of PARKIN and p62/SQSTM1. Cell Death Differ. *22*, 419–432.

Wu, W., Tian, W., Hu, Z., Chen, G., Huang, L., Li, W., Zhang, X., Xue, P., Zhou, C., Liu, L., et al. (2014). ULK1 translocates to mitochondria and phosphorylates FUNDC1 to regulate mitophagy. EMBO Rep. *15*, 566–575.

Xia, M., Gonzalez, P., Li, C., Meng, G., Jiang, A., Wang, H., Gao, Q., Debatin, K.M., Beltinger, C., and Wei, J. (2014). Mitophagy enhances oncolytic measles virus replication by mitigating DDX58/RIG-I-like receptor signaling. J. Virol. *88*, 5152–5164.

Xu, L.G., Jin, L., Zhang, B.C., Akerlund, L.J., Shu, H.B., and Cambier, J.C. (2012). VISA is required for B cell expression of TLR7. J. Immunol. *188*, 248–258.

Yoshizumi, T., Ichinohe, T., Sasaki, O., Otera, H., Kawabata, S., Mihara, K., and Koshiba, T. (2014). Influenza A virus protein PB1-F2 translocates into mitochondria via Tom40 channels and impairs innate immunity. Nat. Commun. *5*, 4713.

Yun, J., Puri, R., Yang, H., Lizzio, M.A., Wu, C., Sheng, Z.H., and Guo, M. (2014). MUL1 acts in parallel to the PINK1/parkin pathway in regulating mitofusin and compensates for loss of PINK1/parkin. eLife *3*, e01958.

Zhang, J., and Ney, P.A. (2009). Autophagy-dependent and -independent mechanisms of mitochondrial clearance during reticulocyte maturation. Autophagy *5*, 1064–1065.

Zhang, G., Zhang, S., Ding, B., Yang, X., Chen, L., Yan, Q., Jiang, Y., Zhong, Y., and Chen, M. (2014). A leucine residue in the C terminus of human parainfluenza virus type 3 matrix protein is essential for efficient virus-like particle and virion release. J. Virol. *88*, 13173–13188.